Coupled-cluster studies of the hyperfine splitting constants of the thioformyl radical

Nicholas D. K. Petraco, Steven S. Wesolowski, Matthew L. Leininger,[a)] and Henry F. Schaefer III
Center for Computational Quantum Chemistry, University of Georgia, Athens, Georgia 30602-2525

(Received 22 October 1999; accepted 7 January 2000)

Hyperfine splitting constants (hfs) of the $\tilde{X}\,^2A'$ electronic ground state of the thioformyl radical (HCS) have been determined at the coupled-cluster level with single, double, and perturbatively applied connected triple excitations [CCSD(T)] using 39 basis sets. Variation of the CCSD(T) hyperfine splittings with basis set was ascertained using a fixed geometry, optimized at the CCSD(T) level with Dunning's correlation-consistent polarized valence quadruple-ζ basis set (cc-pVQZ). Pople basis sets, 6-311G++$(2d,2p)$ and 6-311G++$(3df,3pd)$, give ^{1}H isotropic coupling constants ($^1HA_{iso}$) in good agreement with the experimental vibrationally averaged value of 127.4 MHz, deviating by 5.5 and 9.3 MHz, respectively. Dunning's valence correlation-consistent basis sets (cc-pVDZ, aug-cc-pVDZ, cc-pVTZ, aug-cc-pVTZ, cc-pVQZ, aug-cc-pVQZ) deviate 6.4 MHz (aug-cc-pVQZ) to 14.9 MHz (cc-pVDZ) from the experimental value. The correlation-consistent core valence analogues of these sets give very similar values with deviations from experiment of 7.4 MHz (cc-pCVQZ) to 14.2 MHz (cc-pCVDZ). A direct comparison with the vibrationally averaged experimental value is not precisely possible since the hyperfine splittings are strongly geometry dependent and all theoretical predictions refer to the equilibrium geometry. Small Pople basis sets (3-12G, 6-31G, and 6-311G) give the worst results, deviating by 49.5, 34.1, and 31.8 MHz, respectively. All CCSD(T) ^{1}H A_{iso} values fall below the experimental value. The ^{13}C and ^{33}S hyperfine splittings are not known experimentally, but the equilibrium values are predicted here to be 274.7 MHz (^{13}C) and 21.7 MHz (^{33}S) at the cc-pCVQZ CCSD(T) level of theory. Significantly different values are predicted by density functional theory (DFT) for the ^{13}C and ^{33}S hyperfine splittings. © *2000 American Institute of Physics.* [S0021-9606(00)31613-0]

INTRODUCTION

Impact models of the recent collision of the Shoemaker–Levy 9 comet into Jupiter have required the thioformyl radical (HCS) to be present as an intermediate to account for the wide range of sulfur-containing compounds detected in the Jovian atmosphere.[1–5] Many research groups are attempting to elucidate the nature of the related atomic and molecular collisions in space. However, much remains to be studied in the realm of interstellar sulfur chemistry.[6–10] While several sulfur compounds have been detected in space,[6,11–14] reaction models have struggled to predict consistent values for sulfur abundances.[15–19] Although many detailed reaction mechanisms have yet to be resolved, the ($\tilde{X}\,^2A'$) HCS radical is now established as the major product in the collision of (^3P) C and ($\tilde{X}\,^2A_1$) H_2S—a central reaction in the neutral–neutral molecular synthesis of sulfur compounds.[7] This elementary reaction may also play a key role in sooty flame chemistry as rate constants associated with H_2S and C have been shown in some cases to be competitive with those of molecular and atomic oxygen.[7,20]

The HCS radical was first observed in 1992 by Anacona using far-infrared laser magnetic resonance to monitor the reaction of atomic fluorine with $(CH_3)SH$, $(CH_3)_2S_2$, and $(CH_3)_2S$.[21] In a series of recent articles, Kaiser *et al.* have discussed the dynamics of the (^3P) C plus ($\tilde{X}\,^2A_1$) H_2S reaction which also produces the HCS radical.[5,7,22] Their crossed molecular beam studies indicate H_2SC is first formed and undergoes hydrogen migration to yield thiohydroxycarbene (HCSH). The S–H bond of this species ruptures to give ($\tilde{X}\,^2A'$) HCS and ($^2S_{1/2}$) H.[22] Habara *et al.* subsequently used Fourier transform millimeter-wave spectroscopy to extract fine and hyperfine splitting constants (hfs) of ground state HCS.[8] It should be noted that the experimental splitting constant was inevitably obtained from a vibrationally averaged structure which is inherently different from those obtained in *ab initio* equilibrium treatments. The positive isotropic hyperfine splitting (or Fermi contact term) of 127.4 MHz indicates that HCS is a σ-radical with a singly-occupied a' molecular orbital (SOMO) extending over a large portion of the molecular plane.[8] The analogous ($\tilde{X}\,^2A'$) HCO molecule likewise has a positive Fermi contact term, however with a much larger value, 388.9 MHz, suggesting that HCS has a wider bond angle.[8,23]

Several theoretical studies on HCS have been performed and are summarized in Table I. In 1983 the first *ab initio* examination by Goddard predicted a geometry with r_e(C–H) 1.086 Å, r_e(C–S) 1.570 Å, θ_e(H–C–S) 132.8° using the configuration interaction method including single and double excitations (CISD) coupled with a double-ζ basis set

[a)]Present address: Sandia National Laboratories, MS 9214, Livermore, California 94551-0969.

TABLE I. Equilibrium geometries and harmonic vibrational frequencies[a] of the $\tilde{X}\,^2A'$ state of HCS.

Method	Total energy (hartree)	r_{CH} (Å)	r_{CS} (Å)	θ_e (deg)	$\omega_1(a')$	$\omega_2(a')$	$\omega_3(a')$
DZP CISD[b]		1.086	1.570	132.8	2990	1145	874
DZP MCSCF[c,d]		1.083	1.573	132.8	3209	1178	876
6-31G* MP2[e,f]		1.091	1.512	134.1	⋯	⋯	⋯
6-311G** CISD[g]		1.083	1.557	132.4	3202	1265	875
TZ(2*df*,2*p*) CASSCF[h,i]		1.101	1.582	132.0	3006	1146	886
QZ2P CCSD(T)[j,k]		1.087	1.564	132.3	3146	1218	837
DZP CCSD(T)[l]	−436.246 032	1.102	1.591	129.9	3124	1190	890
TZ2P(*f*,*d*) CCSD(T)[l]	−436.332 281	1.083	1.569	131.4	3163	1203	861
cc-pVQZ CCSD(T)[l]	−436.393 095	1.085	1.558	132.2	3148	1223	836

[a]Frequencies in cm^{-1}.
[b]Goddard (Ref. 24) scaled frequencies.
[c]Senekowitsch *et al.*, Ref. 74.
[d]Multiconfigurational self-consistent field with 19 reference configurations (MCSCF).
[e]Curtiss *et al.*, Ref. 75.
[f]Second-order Møller–Plesset perturbation theory (MP2).
[g]Webster (Ref. 41), frequencies by perturbation theory (Ref. 42).
[h]Clouthier *et al.*, Ref. 9.
[i]Complete active space self-consistent field (CASSCF) considering 11 electrons in 9 valence orbitals.
[j]Kaiser *et al.*, Ref. 22.
[k]Ochsenfeld *et al.*, Ref. 72.
[l]This work.

with polarization functions (DZP).[24] The latest *ab initio* study on HCS by Kaiser *et al.* predicted a remarkably similar geometry of r_e(C–H) 1.087 Å, r_e(C–S) 1.564 Å, θ_e(H–C–S) 132.3° using coupled-cluster methods with single, double, and perturbatively applied connected triple excitations [CCSD(T)] and a much larger quadruple-ζ quality basis set with two sets of polarization functions (QZ2P).[22]

Many studies have noted the sensitivity of hyperfine splittings to geometry, basis set size, and level of theory employed;[25–39] Gauld, Eriksson, and Radom noted for 11 small radicals, agreement within about 10% can be obtained between computed and experimentally determined hyperfine splittings when highly correlated methods and large Pople basis sets are used, e.g., QCISD(T)/6-311+G(2*df*,*p*). They also found that the popular Dunning correlation-consistent basis sets usually gave poorer results due to the highly contracted nature of their core functions.[28] Cramer and Lim found that for 25 systems containing phosphorus, the spin-unrestricted Møller–Plesset second-order perturbation theory (UMP2) method applied at 6-31G*/Hartree–Fock geometries yielded fair agreement with experiment with ^{1}H A_{iso} splittings deviating an average of 38.8 MHz.[35] Density functional theory (DFT) treatments typically produce ^{1}H A_{iso} values in error by about 10–30 MHz for similar small molecular systems.[29–31] A very recent study by Chen and Huang[40] shows that B3LYP isotropic hyperfine constants for HCS are in excellent agreement with experiment, ranging from 127.4–129.1 MHz. It should be noted that the first *ab initio* prediction of ^{1}H A_{iso} for HCS (109.8 MHz) was obtained by Webster at a CISD 6-311G** geometry using a second-order perturbation method developed by Krohn.[41,42] In light of these findings, we have examined all the hyperfine splitting constants for HCS using a wide variety of basis sets and a highly correlated method [CCSD(T)] in order to further elucidate empirical trends and to examine the effects of systematically uncontracting the *s*- and *sp*-spaces. Limited density functional theory hfs calculations were also carried out using the Becke-3/Lee–Yang–Parr (B3LYP) functional using both DFT and CCSD(T) optimized geometries and assorted basis sets.

CONSIDERATIONS FOR HYPERFINE SPLITTING CONSTANTS

The coupling between the spins of an unpaired electron and magnetic atomic nuclei induces a splitting of peaks in an electron spin resonance (ESR) spectrum known as the hyperfine splitting. These splittings are often observed on a number of peaks due to the ''spread'' of a radical electron over a large part of the molecule as it interacts with a number of nuclei.[43] The hfs are thus a useful tool to gauge the extent of the unpaired electron delocalization. These constants may be factored into isotropic (A_{iso}) and anisotropic (A_{aniso}) terms. The isotropic term may be considered a measure of *s* character in the radical electron's molecular orbital.[43] This constant depends explicitly on the local value of the wave function at the nuclei, and is therefore also called the Fermi contact term.[25] The electronic density at the nucleus is related to A_{iso} (popular units in the literature for hfs are megahertz and gauss (2.8025 G=1 MHz)) in the following way:

$$A_{iso}=\frac{8\pi}{3h}g_e\beta_e g_I\beta_N|\Psi_0|^2, \tag{1}$$

where h is Plank's constant, g_e is the electronic *g*-factor, β_e is the Bohr magneton, g_I is the nuclear *g*-factor, β_N is the nuclear magneton, and $|\Psi_0|^2$ is the unpaired electron spin density at the nucleus.

Since *s*-orbitals have no node at the nucleus, the isotropic constant is highly sensitive to the *s*-space orbital description. Unlike Slater-type orbitals, Gaussian functions do not display the proper cusp condition at the nucleus. However, there is some controversy as to whether or not a highly satu-

rated space of *s*-type Gaussian orbitals is needed to reliably predict these values.[25,28,36,44,45] For radicals with singly occupied σ-type orbitals (σ-radicals) the A_{iso} value is positive. Theoretically, the wider a bond angle, the more π-character a singly-occupied molecular orbital (SOMO) contains and the smaller the A_{iso} constant.

COMPUTATIONAL DETAILS

Energies were obtained using spin-unrestricted Hartree–Fock (UHF) reference wave functions combined with coupled-cluster single, double, and perturbatively applied connected triple excitations [CCSD(T)].[46–49] Density functional theory was also employed using the three-parameter HF/DFT hybrid Becke exchange functional,[50] with the correlation functional of Lee, Yang, and Parr (B3LYP).[51] No orbitals were frozen in the CCSD(T) procedures. The ground state $^2A'$ occupation of the HCS radical in C_s symmetry is

$$[\text{core}](6a')^2(7a')^2(8a')^2(2a'')^2(9a')^2(10a').$$

Stationary point geometrical structures were optimized within C_s symmetry constraints using analytic gradient techniques, until residual Cartesian coordinate gradients were less than 10^{-6} a.u. with the exception of optimizations at the cc-pVQZ CCSD(T) level of theory. The latter structure was determined using finite differences of energies while maintaining the 10^{-6} a.u. gradient convergence criterion. The CCSD(T) force constants were determined by finite differences of analytic gradients [DZP and TZ2P(f,d) basis sets] or finite differences of energies (cc-pVQZ basis set) while DFT force constants were determined analytically.

Equilibrium geometries were optimized at the CCSD(T) level using three basis sets. The smallest was a DZP basis consisting of the Huzinaga–Dunning–Hay[52–54] set of contracted Gaussian functions, but with sets of five *d*-type and three *p*-type polarization functions from Dunning and Woon's correlation-consistent double-ζ (cc-pVDZ) basis sets[55,56] centered on the heavy atoms and hydrogen, respectively. The contraction scheme for the set was H($4s1p/2s1p$), C($9s5p1d/4s2p1d$), S($12s8p1d/6s4p1d$). A TZ2P(f,d) basis was formed from the Huzinaga–Dunning[52,57] *sp* sets augmented with two sets of polarization functions from Dunning and Woon's cc-pVTZ sets[55,56] (two sets of five *d*-type functions on S and C and two sets of *p*-type functions on H) as well as a set of seven *f*-type functions on S and C and a set of five *d*-type functions on H. The contraction scheme for this set was H($5s2p1d/3s2p1d$), C($10s5p2d1f/4s3p2d1f$), S($15s9p2d1f/5s4p2d1f$). The largest basis set used for CCSD(T) geometry optimizations was the full cc-pVQZ basis set of Dunning and Woon[55,56] with a contraction scheme of H($6s3p2d1f/4s3p2d1f$), C($12s6p3d2f1g/5s4p3d2f1g$), S($16s11p3d2f1g/6s5p3d2f1g$). The DZP, TZ2P(f,d), and cc-pVQZ basis sets contained 48, 76, and 144 total contracted functions, respectively.

Equilibrium geometries were optimized at the B3LYP level using six basis sets. The basis sets designated 6-311G++($2d,2p$) and 6-311G++($3df,3pd$) were used and formed from the 6-311G basis set of Krishnan *et al.*[58] and McLean *et al.*[59] combined with the polarization and diffuse functions of Frisch *et al.*[60] and Clark *et al.*[61] These basis sets have contraction schemes of H($6s2p/4s2p$), C($12s6p2d/5s4p2d$), S($14s10p2d/7s6p2d$), (72 functions) and H($6s3p1d/4s3p1d$), C($12s6p3d1f/5s4p3d1f$), S($14s10p3d1f/7s6p3d1f$), (104 functions), respectively. The full cc-pVTZ and augmented cc-pVTZ (aug-cc-pVTZ) basis sets of Dunning and Woon[55,56] were used with contraction schemes of H($5s2p1d/3s2p1d$), C($10s5p2d1f/4s3p2d1f$), S($15s9p2d1f/5s4p2d1f$), (78 functions) and H($6s3p2d/4s3p2d$), C($11s6p3d2f/5s4p3d2f$), S($16s10p3d2f/6s5p3d2d$), (119 functions), respectively. The same cc-pVQZ basis sets of Dunning and Woon described above was used as well as their aug-cc-pVQZ basis set with the contraction scheme of H($17s4p3d2f/5s4p3d2f$), C($13s7p4d3f2g/6s5p4d3f2g$), S($17s12p4d3f2g/7s6p4d3f2g$), (210 functions).[55,56]

Hyperfine splittings (hfs) were determined from CCSD(T) and B3LYP spin densities using the optimized CCSD(T) cc-pVQZ geometry and 39 basis sets. The hfs were also obtained using the B3LYP method at the six B3LYP optimized geometries. Single point energy and one electron property calculations were carried out with the standard DZP[52–56] (48 functions), 3-21G[62,63] (24 functions), 6-31G[64,65] (24 functions), 6-311G[58,59] (37 functions), 6-311G++($2d,2p$)[58–61] (72 functions), 6-311G++($3df,3pd$)[58–61] (104 functions), cc-pVDZ (37 functions), aug-cc-pVDZ (59 functions), cc-pCVDZ (50 functions), aug-cc-pCVDZ (72 functions), cc-pVTZ (78 functions), aug-cc-pVTZ (119 functions), cc-pCVTZ (116 functions), aug-cc-pCVTZ (157 functions), cc-pVQZ (144 functions), cc-pCVQZ (223 functions), and aug-cc-pVQZ (210 functions).[55,56,66] The *s*- and *sp*-spaces of the following basis sets were then uncontracted and designated ucs DZP (55 functions), ucsp DZP (73 functions), ucs 3-21G (33 functions), ucsp 3-21G (45 functions), ucs 6-31G (45 functions), ucsp 6-31G (72 functions), ucs 6-311G (52 functions), ucsp 6-311G (70 functions), ucs 6-311G++($2d,2p$) (87 functions), ucsp 6-311G++($2d,2p$) (105 functions), ucs 6-311G++($3df,3pd$) (119 functions), ucsp 6-311G++($3df,3pd$) (137 functions), ucs cc-pVDZ (53 functions), ucsp cc-pVDZ (74 functions), ucs aug-cc-pVDZ (75 functions), ucsp aug-cc-pVDZ (96 functions), ucs cc-pVTZ (96 functions), ucsp cc-pVTZ (117 functions), ucs aug-cc-pVTZ (137 functions), ucsp aug-cc-pVTZ (158 functions), ucs cc-pVQZ (163 functions), and ucsp cc-pVQZ (187 functions).

Spin densities used to determine hyperfine splitting constants were computed at the CCSD(T) levels utilizing the analytical coupled-cluster relaxed density.[25,49,67–69] All CCSD(T) and DFT computations were carried out using the ACES II (Ref. 70) and GAUSSIAN 94 (Ref. 71) program packages, respectively.

RESULTS AND DISCUSSION

Geometry and frequencies

All optimized geometries and vibrational frequencies are listed in Tables I and II. The CCSD(T) bond lengths and

TABLE II. B3LYP equilibrium geometries for the $\tilde{X}\,^2A'$ state of HCS.

Basis set	r_{CH} (Å)	r_{CS} (Å)	θ_e (deg)
6-311G++(2*d*,2*p*)	1.088	1.562	131.6
6-311G++(3*df*,3*pd*)	1.088	1.557	132.5
cc-pVTZ	1.088	1.563	131.9
aug-cc-pVTZ	1.088	1.563	132.0
cc-pVQZ	1.087	1.559	132.3
aug-cc-pVQZ	1.087	1.559	132.3

angle change less than 0.01 Å and 0.8° when the basis set is increased from TZ2P(*f*,*d*) to cc-pVQZ, suggesting that the geometry will change very little upon further extension of the basis set. The same conclusion may be reached upon examination of the B3LYP optimized geometries. The B3LYP bond lengths and angle change less than 0.01 Å and 0.7°, respectively. Computations using CCSD(T) and the cc-pVQZ basis set represent the highest level of theory for which optimized geometries and harmonic vibrational frequencies were obtained. As expected, the theoretical parameters at this level almost match those found by Kaiser *et al.* and Ochsenfeld *et al.* at the QZ2P CCSD(T) level.[22,72] Although no experiment has been performed to precisely determine the structural parameters of the HCS radical, the consistency with previous calculations and the high level of theory employed suggest experimental techniques would yield very similar values. The theoretical geometries are in agreement with the qualitative experimental deductions of Habara *et al.*, i.e., HCS has a bent structure with C_s symmetry.[8]

Energetics

Energy determinations were *not* obtained within the frozen core approximation. While this leads to geometries in good agreement with previous results, as can be seen from the single point energies listed in Tables III, IV, V, and VI the energetic results can be a bit anomalous when comparing Dunning valence correlation consistent basis sets (cc-pVXZ) to Pople basis sets. For example the cc-pVQZ basis set with 144 functions yields an energy 0.0676 hartree (42.4 kcal/mol) higher than the 6-311G++(3*df*,3*pd*) basis set with only 104 functions, at the cc-pVQZ CCSD(T) optimized geometry. Upon freezing the six core functions of cc-pVQZ and the six core along with the highest virtual orbital of 6-311G++(3*df*,3*pd*), the former produces an energy lower by 0.0327 hartree (20.5 kcal/mol) consistent with the expected trend. The energies listed in Table VII demonstrate that upon freezing core and high-lying virtual orbitals, at the cc-pVQZ CCSD(T) optimized geometry the selected basis sets produce lower energies as the number of functions increases. The Dunning valence correlation-consistent basis sets were expressly constructed using the frozen core approximation and not deleting any virtual orbitals.[55,56] Thus using the frozen core/virtual approximation yields good optimized geometries and relative energetics. However, hyperfine splittings are core electron properties, and there is no theoretical basis for freezing core when obtaining these values.

TABLE III. Isotropic hyperfine splitting (MHz) computed with the CCSD(T) method using small Pople basis sets for the $\tilde{X}\,^2A'$ state of HCS at the cc-pVQZ/CCSD(T) optimized geometry.

Basis	Total energy (hartree)	^{1}H	^{13}C	^{33}S
3-21G	−433.867 677	77.91	326.21	17.54
ucs 3-21G	−434.286 895	78.67	282.87	15.76
ucsp 3-21G	−434.436 273	79.86	279.53	16.05
6-31G	−435.982 103	93.33	379.29	24.45
ucs 6-31G	−436.035 062	91.38	343.64	20.41
ucsp 6-31G	−436.202 969	93.11	335.01	21.09
6-311G	−436.155 522	95.68	340.02	20.42
ucs 6-311G	−436.169 150	94.87	335.86	22.43
ucsp 6-311G	−436.231 981	95.33	335.50	22.81
Expt.[a]		127.43	⋯	⋯

[a]Experimentally determined (vibrationally averaged) isotropic hyperfine coupling constant (Ref. 8).

TABLE IV. Isotropic hyperfine splitting (MHz) computed with the CCSD(T) method using Dunning basis sets for the $\tilde{X}\,^2A'$ state of HCS at the cc-pVQZ/CCSD(T) optimized geometry.

Basis	Total energy (hartree)	^{1}H	^{13}C	^{33}S
DZP	−436.244 860	120.06	304.51	19.82
ucs DZP	−436.249 174	112.82	283.95	22.75
ucsp DZP	−436.375 216	113.58	277.01	22.66
cc-pVDZ	−436.189 001	112.50	294.38	27.60
ucs cc-pVDZ	−436.232 485	110.18	288.35	21.84
ucsp cc-pVDZ	−436.393 190	111.28	283.40	21.48
aug-cc-pVDZ	−436.208 095	114.61	276.68	32.83
ucs aug-cc-pVDZ	−436.251 599	112.96	271.55	25.31
ucsp aug-cc-pVDZ	−436.410 405	113.93	267.93	24.91
cc-pVTZ	−436.325 650	118.68	248.19	29.40
ucs cc-pVTZ	−436.356 811	116.80	271.91	23.12
ucsp cc-pVTZ	−436.494 760	117.55	271.89	23.30
aug-cc-pVTZ	−436.337 303	119.68	246.99	29.48
ucs aug-cc-pVTZ	−436.365 813	117.56	265.11	24.31
ucsp aug-cc-pVTZ	−436.501 286	118.26	265.12	24.49
cc-pVQZ	−436.393 095	120.05	266.70	23.80
ucs cc-pVQZ	−436.415 938	120.49	273.52	23.51
ucsp cc-pVQZ	−436.536 906	121.13	273.95	23.40
aug-cc-pVQZ	−436.396 845	121.06	263.95	23.69
Expt.[a]		127.43	⋯	⋯

[a]Experimentally determined (vibrationally averaged) isotropic hyperfine coupling constant (Ref. 8).

TABLE V. Isotropic hyperfine splitting (MHz) computed with the CCSD(T) method using Dunning core valence correlation-consistent basis sets for the $\tilde{X}\,^2A'$ state of HCS at the cc-pVQZ/CCSD(T) optimized geometry.

Basis	Total energy (hartree)	^{1}H	^{13}C	^{33}S
cc-pCVDZ	−436.434 025	113.21	279.19	27.84
aug-cc-pCVDZ	−436.453 107	115.22	263.58	33.16
cc-pCVTZ	−436.663 745	118.47	272.90	18.56
aug-cc-pCVTZ	−436.670 502	119.34	265.42	19.69
cc-pCVQZ	−436.741 131	120.07	274.74	21.69
Expt.[a]		127.43	⋯	⋯

[a]Experimentally determined (vibrationally averaged) isotropic hyperfine coupling constant (Ref. 8).

TABLE VI. Isotropic hyperfine splitting (MHz) computed with the CCSD(T) method using large Pople basis sets for the $\tilde{X}\,^2A'$ state of HCS at the cc-pVQZ/CCSD(T) optimized geometry.

Basis	Total energy (hartree)	^{1}H	^{13}C	^{33}S
6-311G++(2*d*,2*p*)	−436.378 706	121.96	265.59	20.28
ucs 6-311G++(2*d*,2*p*)	−436.390 830	119.57	263.60	23.45
ucsp 6-311G++(2*d*,2*p*)	−436.453 844	120.00	263.46	23.85
6-311G++(3*df*,3*pd*)	−436.460 718	118.17	263.39	20.91
ucs 6-311G++(3*df*,3*pd*)	−436.471 805	116.79	262.01	24.21
ucsp 6-311G++(3*df*,3*pd*)	−436.535 081	117.14	261.61	24.71
Expt.[a]		127.43	···	···

[a]Experimentally determined (vibrationally averaged) isotropic hyperfine coupling constant (Ref. 8).

Hyperfine splittings

CCSD(T) hydrogen isotropic splittings

Theoretically determined values for the isotropic portions of the ^{1}H, ^{13}C, and ^{33}S hyperfine splitting constants obtained using CCSD(T) spin densities appear in Tables III, IV, V, and VI. Focusing on the isotropic values for ^{1}H ($^1H\,A_{iso}$), Figure 1 illustrates that there is no well-defined relationship between accuracy and basis set sophistication, other than the fact that very large basis sets are in general better than very small sets. There are, however, four groups of basis sets which give similar results.

The first group contains the smaller standard Pople basis sets consisting of 3-21G, 6-31G, and 6-311G and their uncontracted *s* and *sp* counterparts listed in Table III. These sets on the whole yield the worst results compared to experiment; however this might be expected due to their poor description of the *s*-space.[25] The ^{1}H A_{iso} vary from the vibrationally averaged experimental value of 127.4 MHz by 31.8 MHz (6-311G, 24.9%)–49.5 MHz (3-21G, 38.9%). As basis set size increases, uncontracting the *s*-space slightly degrades the accuracy with deviations from experiment of 31.8–48.8 MHz (25.6%–38.3%). Uncontraction of the *sp*-space however shifts the values narrowly toward experiment with deviations from 32.1–47.6 MHz (25.2%–37.3%) with increasing basis set size.

The Dunning valence correlation-consistent basis sets (cc-pVDZ, aug-cc-pVDZ, cc-pVTZ, aug-cc-pVTZ, cc-pVQZ, aug-cc-pVQZ) and their uncontracted analogs are listed in Table IV. The ^{1}H A_{iso} values deviate by 14.9 (11.7%), 12.8 (10.1%), 8.8 (6.7%), 7.8 (6.1%), 7.1 (5.8%), and 6.4 MHz (5.0%), respectively, with the aug-cc-pVQZ basis set yielding the value in best agreement with experiment, 121.1 MHz. Within this group, as basis set size increases the ^{1}H A_{iso} converges toward the experimental result. The largest improvement comes from moving from the aug-cc-pVDZ to the cc-pVTZ basis set, with a difference between these two consecutive basis sets of about 4 MHz. However the difference between any two other consecutive Dunning valence correlation-consistent basis sets is only about 1–2 MHz. Uncontracting the *s*-space slightly degrades the agreement with experiment, with deviations from 6.9 MHz (ucs cc-pVQZ, 5.4%)–17.3 MHz (ucs cc-pVDZ, 13.5%). A similar situation is found when uncontracting the *sp*-space (for all but the aug-cc-pVQZ basis set). As basis set size increases deviations range from 6.3 MHz (ucsp cc-pVQZ, 4.9%)–16.2 MHz (ucsp cc-pVDZ, 12.7%). The ucsp cc-pVQZ basis set performs roughly as well as the aug-cc-pVQZ basis set. Surprisingly, the small DZP basis set does quite well, coming within 5.8% or 7.4 MHz of experiment. The difference decreases to 11.5%, 14.6 MHz and 10.9%, 13.9 MHz when uncontracting the *s*- and *sp*-spaces respectively; however this success is most likely due to fortuitous cancellation of errors.[26,28]

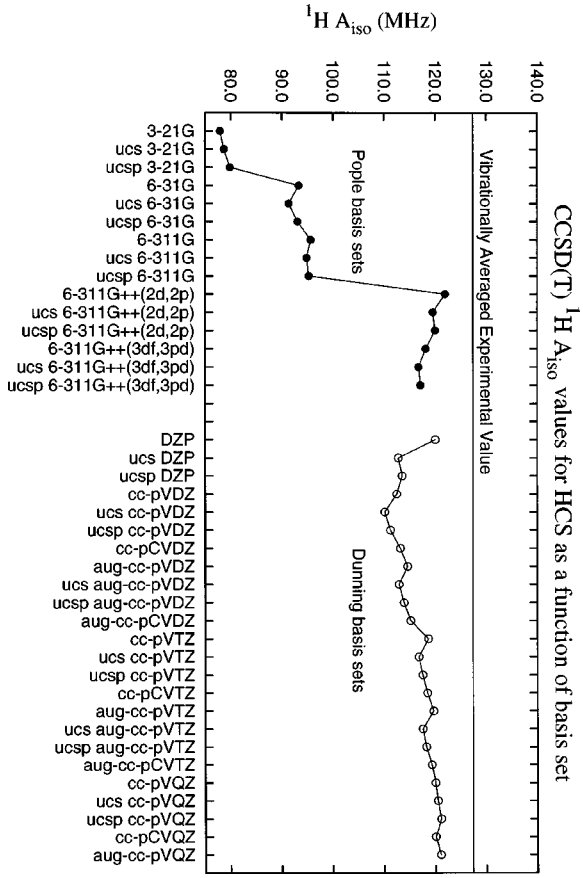

FIG. 1. Variation of the equilibrium CCSD(T) ^{1}H A_{iso} values as a function of basis set. The vibrationally averaged experimental value (shown as the solid horizontal line) has a value of 127.4 MHz. All hyperfine constants were computed at the cc-pVQZ/CCSD(T) optimized geometry.

TABLE VII. The CCSD(T) energies for $\tilde{X}\,^2A'$ HCS computed at the cc-pVQZ CCSD(T) optimized geometry employing the frozen core approximation (cor=core functions frozen, vir=virtual functions frozen).

Basis	Number of functions	Total energy (hartree)
6-311G++(2*d*,2*p*) 6 cor/1 vir	72	−436.226 599
6-311G++(3*df*,3*pd*) 6 cor/1 vir	104	−436.273 375
cc-pVDZ 6 cor	37	−436.180 773
aug-cc-pVTZ 6 cor	59	−436.208 095
cc-pVTZ 6 cor	78	−436.277 299
aug-cc-pVTZ 6 cor	119	−436.283 897
cc-pVQZ 6 cor	144	−436.306 054
aug-cc-pVQZ 6 cor	210	−436.308 618

The third group consisted of the Dunning core valence correlation-consistent basis sets listed in Table V (cc-pCVDZ, aug-cc-pCVDZ, cc-pCVTZ, aug-cc-pCVTZ, cc-pCVQZ). These cc-pCVXZ basis sets yielded ^{1}H A_{iso} values very close to those yielded by the cc-pVXZ basis sets. The results make sense in light of the fact that the basis set for hydrogen is the same for both groups. These splittings vary from experiment by 7.4 MHz (cc-pCVQZ, 5.8%)–14.2 MHz (cc-pCVDZ, 11.2%). The *s*- and *sp*-spaces of these basis sets were not uncontracted due to severe linear dependency problems.

Finally the ^{1}H A_{iso} hfs obtained with the large Pople basis sets appear in Table VI. The 6-311G++$(2d,2p)$ gives the closest agreement (122.0 MHz) using CCSD(T), deviating by only 5.5 MHz (4.3%) from experiment. The larger 6-311G++$(3df,3pd)$ Pople basis set does about as well as the aug-cc-pVTZ Dunning basis set yielding a ^{1}H A_{iso} value of 118.2 MHz, deviating from experiment by 9.3 MHz or 7.3%. Uncontracting the *s*- and *sp*-spaces for these basis sets slightly decreases the agreement with experiment as can be seen from Table VI. Gauld, Eriksson, and Radom found similar results for ^{1}H A_{iso} with larger contracted Pople basis sets for assorted radical species.[28] However, upon uncontracting the *s*- and *sp*-spaces they noted moderate improvement or no change of results. They also obtained relatively poorer hfs values with the Dunning correlation-consistent basis sets. Results changed little when *s*- and *sp*-spaces were uncontracted and did not necessarily improve the ^{1}H A_{iso}.[28] However, the large basis set CCSD(T) values are a significantly improved relative to the constant obtained by Webster (109.8 MHz) at a CISD 6-311G** geometry using second-order perturbation theory techniques.[41,42]

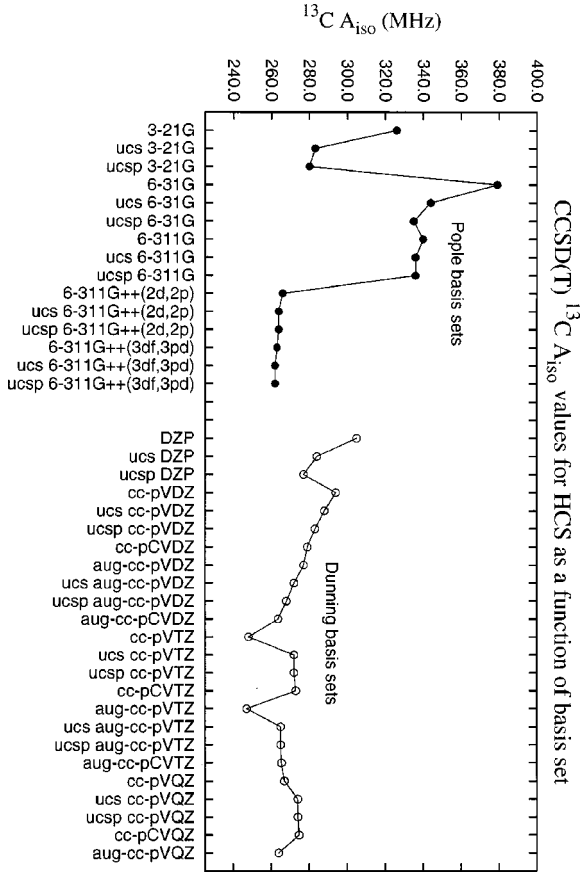

FIG. 2. Variation of the CCSD(T) ^{13}C A_{iso} values as a function of basis set. All hyperfine constants were computed at the cc-pVQZ/CCSD(T) optimized geometry.

CCSD(T) carbon isotropic splittings

Focusing on the Fermi contact terms for the ^{13}C and ^{33}S nuclei, the reliability of the theoretical results and the effects of basis set uncontraction are more difficult to judge due to the lack of experimental data. Quantitative accuracy for ^{13}C hyperfine constants has been demonstrated for a number of diatomic systems in the literature. For example, Fernández *et al.* found A_{iso} constants within 2 MHz of experiment for $\tilde{X}\ ^2\Sigma^+$ CN and CP using a complete active space wave function and an uncontracted *sp*-space Dunning correlation-consistent basis set.[26] In their systematic diatomic study, uncontraction of the *sp*-space was found to be critical. However, Fig. 2 illustrates that our CCSD(T) ^{13}C hyperfine constants show extremely large variation which severely limits its prediction of an experimental value. The effect of *s* and *sp* uncontraction is much more visible in this case relative to that for hydrogen. However, the large Pople-type sets again show an invariance to uncontraction and produce the most consistent results with ^{13}C A_{iso} values ranging from 261.6 MHz [ucsp6-311G++$(3df,3pd)$]–265.6 MHz [6-311G++$(2d,2p)$]. The Dunning valence correlation-consistent basis set values vary significantly more than those produced by the large Pople sets with constants ranging from 247.0 MHz (aug-cc-pVTZ)–294.4 MHz (cc-pVDZ). There is some indication that these basis sets will converge on some value as the predicted ^{13}C A_{iso} seem to settle past ucs aug-cc-pVTZ and approach those yielded by the large Pople sets, with values ranging from 264.0 MHz (aug-cc-pVQZ)–274.0 MHz (ucsp cc-pVQZ). The ^{13}C A_{iso} produced by the Dunning core valence basis sets do not vary as wildly as their valence basis set counterparts with values ranging from 263.6 MHz (aug-cc-pCVDZ)–279.2 MHz (cc-pCVDZ). Notable is that as *s*- and *sp*-spaces are uncontracted within the valence correlation-consistent basis sets, the ^{13}C A_{iso} values approach those yielded by the core valence analogues. Also, as the number of functions increase for the contracted valence correlation consistent basis sets, this A_{iso} value approaches that yielded by the core valence analogue. It is reasonable to expect the true ^{13}C hyperfine constant for HCS to fall near 264 MHz with an error of perhaps ± 10 MHz.

CCSD(T) sulfur isotropic splittings

Figure 3 shows the variation of ^{33}S A_{iso} with the number of functions in the basis set. Here the largest effects of uncontraction are observed as even the values using large Pople basis sets are significantly altered. The smaller 6-311G Pople basis set interestingly predicts a value (20.4 MHz) in line with those obtained using the larger Pople basis sets, [20.3 MHz,6-311G++$(2d,2p)$;20.9 MHz 6-311G++$(3df,3pd)$] unlike for ^{1}H and ^{13}C A_{iso}. Note too that the valence and core valence correlation-consistent Dunning sets seem to predict relatively invariant values past ucs aug-

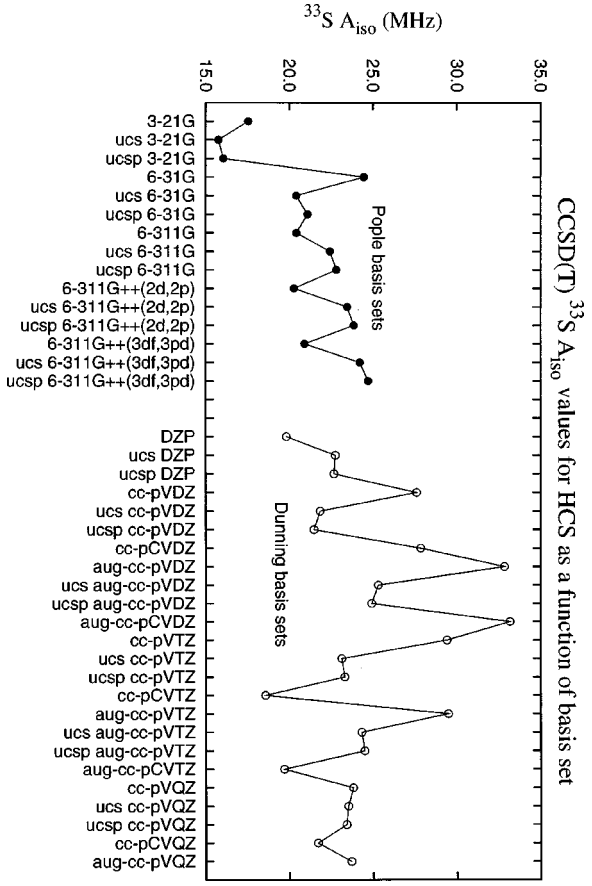

FIG. 3. Variation of the CCSD(T) ^{33}S A_{iso} values as a function of basis set. All hyperfine constants were computed at the cc-pVQZ/CCSD(T) optimized geometry.

cc-pVTZ, (19.7 MHz, aug-cc-pCVTZ–24.5 MHz, ucsp aug-cc-pVTZ) and gravitate towards the large Pople basis set predictions, similar to the trends observed for ^{13}C A_{iso}. Again, however, with such wide scatter an estimate of the true hyperfine splitting may be placed at around 24 $\pm$10 MHz.

Density functional isotropic splittings

Considering the widespread application of density functional theory to compute hfs,[28–30,40,73] we chose to carry out DFT computations on the ^{1}H, ^{13}C, and ^{33}S A_{iso} hfs using B3LYP spin densities at B3LYP optimized geometries within the 6-311G++$(2d,2p)$, 6-311++G$(3df,3pd)$, cc-pVTZ, aug-cc-pVTZ, cc-pVQZ, and aug-cc-pVQZ basis sets. The DFT hfs values computed at the B3LYP optimized geometry will be referred to as B3LYP/B3LYP. The same A_{iso} values were also computed with B3LYP using the cc-pVQZ CCSD(T) optimized geometry and the same basis sets. These values are designated B3LYP/CCSD(T). Results appear in Tables VIII and IX, respectively.

The B3LYP/CCSD(T) treatments yield ^{1}H A_{iso} ranging from 123.1–127.4 MHz, in very close agreement with the vibrationally averaged experimental value of 127.43 MHz. The large Pople basis sets perform about as well as the Dunning sets, and the aug-cc-pVQZ basis produces the the ^{1}H A_{iso} in closest agreement with experiment, 127.4 MHz. As a test, B3LYP ^{1}H A_{iso} values were computed using the cc-pVQZ CCSD(T) geometry and the Pople basis sets that gave the *worst* results using CCSD(T) spin densities (3-21G and 6-31G). The constants were found to be 97.8 and 116.4 MHz, respectively, and illustrate the importance of using an adequate basis set even for DFT treatments. Consistent with the work of Chen and Huang,[40] the B3LYP/B3LYP ^{1}H A_{iso} values are in superb agreement with experiment with values ranging from 122.7 to 127.8 MHz. The Dunning basis sets produce very consistent values, and the aug-cc-pVQZ result of 127.6 MHz shows that the DFT results of Chen and Huang remain steady upon advancement toward the basis set limit.

As can be seen from Tables VIII and IX for a given Dunning valence correlation-consistent or large Pople basis set ^{13}C and ^{33}S A_{iso} values computed with DFT are very close between the CCSD(T) cc-pVQZ geometry and B3LYP geometries. Values differ by only 1–4 MHz for ^{13}C A_{iso} and 0.1–1 MHz for ^{33}S A_{iso} within a given basis set. The situation is somewhat different when comparing these values yielded by CCSD(T) vs. DFT. The Dunning core valence correlation-consistent basis sets yield constants in reasonable agreement with both the B3LYP/B3LYP and B3LYP/CCSD(T) sets of data, within 1–8 MHz for ^{13}C A_{iso} and 0.5–7 MHz for ^{33}S A_{iso}. However, within a given Dunning valence correlation-consistent or large Pople basis set, CCSD(T) predicts ^{13}C A_{iso} to be 14.3 MHz [6-311G++$(3df,3pd)$]–19.4 MHz (aug-cc-pVTZ) *lower* than the B3LYP/CCSD(T) values. The B3LYP/B3LYP constants dis-

TABLE VIII. B3LYP isotropic hyperfine splittings (MHz) computed using the cc-pVQZ CCSD(T) optimized geometry for the $\tilde{X}\,^{2}A'$ state of HCS.

Basis	Total energy (hartree)	^{1}H	^{13}C	^{33}S
3-21G	−434.618 643	97.76	303.89	13.39
6-31G	−436.759 270	116.38	352.18	18.85
6-311G++$(2d,2p)$	−436.849 619	124.63	280.00	8.86
6-311G++$(3df,3pd)$	−436.855 137	123.11	277.73	9.75
cc-pVTZ	−436.856 686	123.92	270.37	19.01
aug-cc-pVTZ	−436.857 983	125.08	266.39	18.91
cc-pVQZ	−436.864 485	126.07	281.85	14.65
aug-cc-pVQZ	−436.865 001	127.35	279.45	14.36
Expt.[a]		127.43	⋯	⋯

[a]Experimentally determined (vibrationally averaged) isotropic hyperfine coupling constant (Ref. 8).

TABLE IX. B3LYP isotropic hyperfine splittings (MHz) using B3LYP optimized geometries for the $\tilde{X}\,^{2}A'$ state of HCS.

Basis	Total energy (hartree)	^{1}H	^{13}C	^{33}S
6-311G++$(2d,2p)$	−436.849 643	127.77	284.38	8.78
6-311G++$(3df,3pd)$	−436.855 145	122.65	277.09	9.78
cc-pVTZ	−436.856 718	126.15	274.16	18.95
aug-cc-pVTZ	−436.858 007	126.84	269.52	18.85
cc-pVQZ	−436.864 490	126.53	282.70	14.64
aug-cc-pVQZ	−436.865 006	127.62	280.05	14.35
Expt.[a]		127.43	⋯	⋯

[a]Experimentally determined (vibrational averaged) isotropic hyperfine coupling constant (Ref. 8).

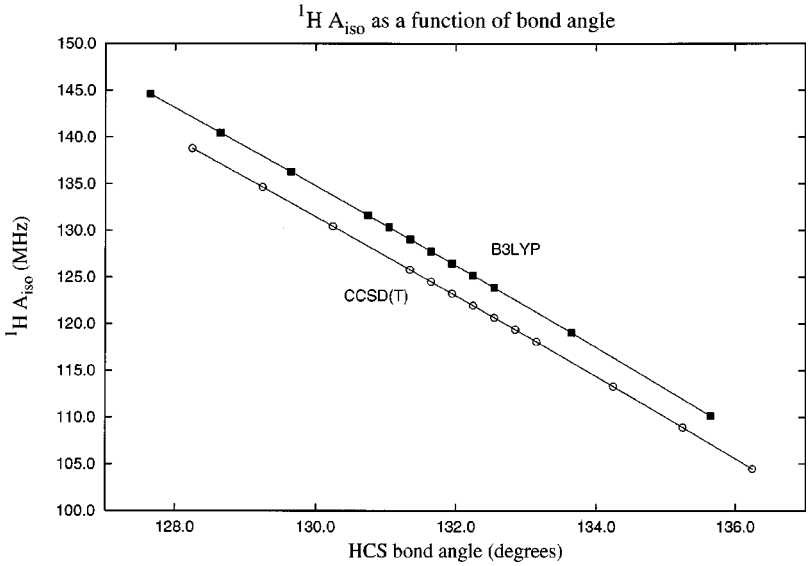

FIG. 4. Variation of the CCSD(T) and B3LYP ^{1}H A_{iso} values as a function of HCS bond angle. Spin densities used to determine the hyperfine splittings were determined using the 6-311G++$(2d,2p)$ basis set. Angle perturbations were made with respect to the cc-pVQZ/CCSD(T) optimized geometry for CCSD(T) values and from the 6-311G++$(2d,2p)$/B3LYP optimized geometry for the the B3LYP values. The bond distances were held fixed in both cases.

agree with the CCSD(T) anywhere from 13.7–26.0 MHz. The high level CCSD(T) value (264.0 MHz, aug-cc-pVQZ) is surprisingly 16.1 MHz lower than the the highest level B3LYP value (280.1 MHz, aug-cc-pVQZ). The disagreement is even worse when comparing the ^{33}S A_{iso} produced by DFT to those obtained with CCSD(T). The differences within a given basis set range from 9.3 MHz (aug-cc-pVQZ)–11.5 MHz [6-311G++$(2d,2p)$] which represents a disparity on the order of 39.4% to 56.7% for CCSD(T) values compared to B3LYP/B3LYP values. The disagreement is about the same between CCSD(T) and B3LYP/CCSD(T).

For this system DFT performs extremely well when comparison is made to experiment for ^{1}H A_{iso}, but this is not always the case.[28,30,31,73] The remarkable agreement of the DFT hyperfine splittings with experiment should be taken with at least three very large grains of salt: (i) DFT ^{1}H hyperfine constants can be in error by as much as 30 MHz,[28–31] (ii) the experimental value has been determined from a *vibrationally averaged* structure, and (iii) the ^{13}C and ^{33}S A_{iso} obtained with CCSD(T) vastly contrast those computed with DFT. Analogous to the work of Chen and Huang,[40] Fig. 4 illustrates the near linear relationship of ^{1}H A_{iso} and the bond angle using the 6-311G++$(2d,2p)$ basis set for both the CCSD(T) and B3LYP data. Note that small perturbations of the equilibrium bond angle (on the order of 1.0°) change the ^{1}H hfs by 5 MHz. Figure 5 demonstrates how, with the same perturbation in the HCS bond angle ^{13}C A_{iso} vary about the same amount. With such variations, it is not at all clear that the DFT results are in any sense ''better'' than the CCSD(T) values since neither incorporates the effects of vibrational averaging. In fact, the CCSD(T) could very well be in *closer* agreement with a hyperfine constant determined from a structure which is not vibrationally averaged.

Typically, triatomic radicals with larger bond angles have smaller Fermi contact terms due to the increased π-character of the singly occupied molecular orbital (SOMO). This generalization should follow for heavy atom isotropic hyperfine splittings as well. Figures 5 and 6 show plots analogous to Fig. 4 for ^{13}C A_{iso} and ^{33}S A_{iso}, respectively. Note that both CCSD(T) and DFT predict a mono-

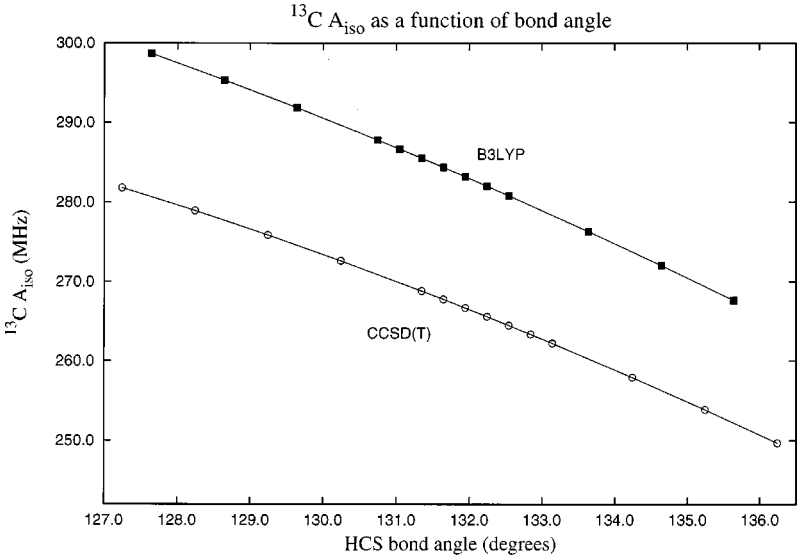

FIG. 5. Variation of the CCSD(T) and B3LYP ^{13}C A_{iso} values as a function of HCS bond angle. The plot was constructed using the same procedure as for Fig. 4.

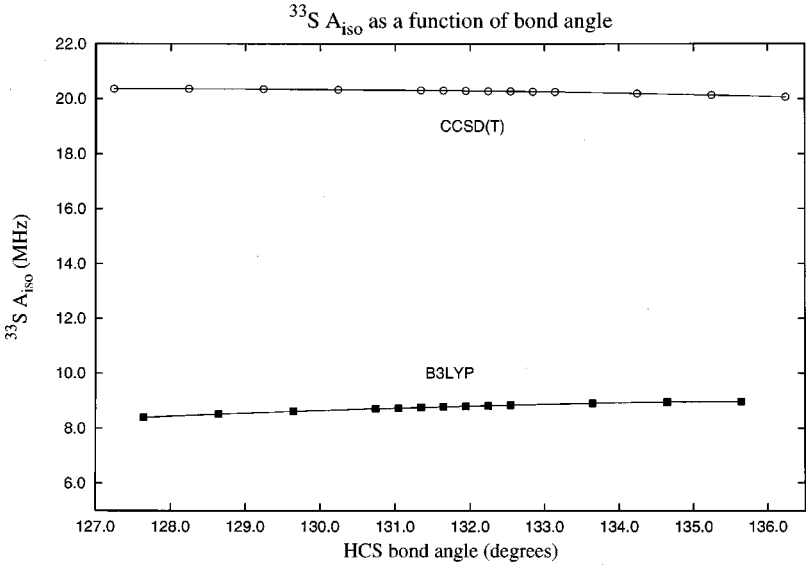

FIG. 6. Variation of the CCSD(T) and B3LYP ^{33}S A_{iso} values as a function of HCS bond angle. The plot was constructed using the same procedure as for Fig. 4.

tonic decrease in the ^{13}C A_{iso} value as the HCS bond angle is increased, similar to the behavior for ^{1}H A_{iso}. Density functional theory however predicts the ^{33}S A_{iso} to *increase* slightly as bond angle is increased, counter to CCSD(T) predictions and chemical intuition. From this result it could be gathered that CCSD(T) perhaps yields isotropic values closer to reality for the heavy atoms. In any event, it is clear that CCSD(T) with a large Pople or Dunning correlation-consistent basis set can describe the spin density well enough to achieve semiquantitative agreement with the experimental vibrationally averaged ^{1}H A_{iso}.

COMPARISONS TO ANALOGOUS RADICALS

Finally, we compared the geometries and hydrogen hyperfine splittings of HCS with the experimental values available for its silicon and oxygen analogs, namely HCO, HSiO, and HSiS. These parameters are summarized in Table X. Perhaps most striking is the sharp variation in the hfs values which range from 451 MHz for HSiO to 127 MHz for HCS. Habara *et al.*[8] and Huang and Chen[40] also noted the surprisingly small ^{1}H A_{iso} value for HCS relative to HCO. The hfs changes by over 260 MHz from HCO to HCS, while HSiO and HSiS are separated by only 116 MHz. Historically, ^{1}H hyperfine splittings have been shown to be very sensitive to geometry, particularly any parameter which affects the hybridization of the molecule.[27,28,40] As stated earlier, triatomic radicals with larger bond angles usually have smaller Fermi contact terms. The trend for ^{1}H A_{iso} is observed in Fig. 4 as well as in the molecules analogous to HCS listed in Table X. Reexamination of the differences in bond angle and hfs for HSiO and HSiS shows that a 2.0° increase in the angle results in a 116 MHz decrease in the hyperfine splitting. As a first approximation, the hyperfine value for HCS might be predicted using a simple proportion of the change in bond angle and the change in the hfs. Since the bond angle increases by 4.8° from HCO to HCS, the estimated hfs value for HCS would decrease by 277 MHz. The result of 111 MHz is in qualitative agreement with the experimental value of 127 MHz and further justifies the rather small value for HCS.

TABLE X. Experimental geometrical parameters and ^{1}H Fermi contact terms of selected molecules.

Molecule	θ_e (deg)	^{1}H A_{iso} (MHz)
HSiO[a]	116.8	451.3
HSiS[b]	118.8	335.7
HCO[c,d]	127.4	388.9
HCS[e]	(132.2)[f]	127.4

[a]Izuha *et al.*, Ref. 76.
[b]Brown *et al.*, Ref. 77.
[c]Austin *et al.*, Ref. 78.
[d]Blake *et al.*, Ref. 23.
[e]Habara *et al.*, Ref. 8.
[f]The cc-pVQZ/CCSD(T) prediction.

CONCLUSIONS

Basis set effects on high level coupled-cluster hyperfine constants have been illustrated. Systematic uncontraction of the *s*- and *sp*-spaces has little impact on the hydrogen isotropic hyperfine splittings, although such expansion of these spaces may be important in other radicals. Large Pople and Dunning type basis sets consistently yield ^{1}H A_{iso} values within 10 MHz of experiment. Given the strong variation of hyperfine splittings with bond angle, this is as good agreement as might be expected between equilibrium predictions (theory) and the observed vibrationally averaged result. The ^{13}C and ^{33}S A_{iso} values show larger fluctuations and sensitivity to the uncontraction of *s* and *p*-functions and to the addition of diffuse basis functions.

ACKNOWLEDGMENTS

This research was supported by the United States National Science Foundation, Grant No. CHE-9815397. The authors are greatful to Dr. K. A. Peterson, Dr. D. F. Feller, Dr. T. H. Dunning, and Professor L. Radom for providing core valence correlation-consistent basis sets for sulfur prior

to publication and for elucidating some basis set trends in frozen core calculations. N.D.K.P. would like to acknowledge J. C. Rienstra-Kiracofe and Dr. Y. Yamaguchi for many valuable discussions.

[1] K. S. Noll, M. A. McGrath, L. M. Trafton, S. K. Atreya, J. J. Caldwell, H. A. Weaver, R. V. Yelle, C. Barnet, and S. Edgington, Science **267**, 1307 (1995).
[2] R. V. Yelle and M. A. McGrath, Icarus **119**, 90 (1996).
[3] K. Zahnle, M.-M. M. Low, K. Lodders, and B. Fegley, Geophys. Res. Lett. **22**, 1593 (1995).
[4] J. I. Moses, M. Allen, and G. R. Gladstone, Geophys. Res. Lett. **22**, 1597 (1995).
[5] R. I. Kaiser, C. Ochsenfeld, M. Head-Gordon, and Y. T. Lee, Science **279**, 1181 (1998).
[6] H. Suzuki, S. Yamamoto, M. Ohishi, N. Kaifu, S. I. Ishikawa, Y. Hirahara, and S. Takano, Astrophys. J. **392**, 551 (1992).
[7] R. I. Kaiser, W. Sun, and A. G. Suits, J. Chem. Phys. **102**, 5288 (1997).
[8] H. Habara, S. Yamamoto, C. Ochsenfeld, M. Head-Gordon, R. I. Kaiser, and Y. T. Lee, J. Chem. Phys. **108**, 8859 (1998).
[9] D. J. Clouthier and R. S. Grev, J. Am. Chem. Soc. **120**, 9386 (1998).
[10] R. I. Kaiser, C. Ochsenfeld, D. Stranges, M. Head-Gordon, and Y. T. Lee, Faraday Discuss. **109**, 183 (1998).
[11] Y. Hirahara, H. Suzuki, S. Yamamoto, K. Kawaguchi, N. Kaifu, M. Ohishi, S. Takano, S. I. Ishikawa, and A. Masuda, Astrophys. J. **394**, 539 (1992).
[12] S. Yamamoto, S. Saito, K. Kawaguchi, N. Kaifu, H. Suzuki, and M. Ohishi, Astrophys. J. **317**, L119 (1987).
[13] S. Saito, K. Kawaguchi, S. Yamamoto, M. Ohishi, H. Suzuki, and N. Kaifu, Astrophys. J. **317**, 115 (1987).
[14] J. Cernicharo, M. Guélin, H. Hein, and C. Kahane, Astron. Astrophys. **181**, L9 (1987).
[15] M. Oppenheimer and A. Dalgarno, Astrophys. J. **187**, 213 (1974).
[16] G. D. Watt and S. B. Charnley, Mon. Not. R. Astron. Soc. **213**, 157 (1985).
[17] E. Herbst, D. J. DeFrees, and W. Koch, Mon. Not. R. Astron. Soc. **237**, 1057 (1989).
[18] D. A. Howe and T. J. Millar, Mon. Not. R. Astron. Soc. **244**, 444 (1990).
[19] T. J. Millar and E. Herbst, Astron. Astrophys. **231**, 466 (1990).
[20] P. R. Wesmoreland, A. M. Dean, J. B. Howard, and J. P. Longwell, J. Phys. Chem. **93**, 8171 (1989).
[21] R. Anacona, J. Chem. Soc., Faraday Trans. **88**, 1507 (1992).
[22] R. I. Kaiser, C. Ochsenfeld, M. Head-Gordon, and Y. T. Lee, J. Chem. Phys. **110**, 2391 (1999).
[23] G. A. Blake, K. V. L. N. Sastry, and F. C. DeLucia, J. Phys. Chem. **80**, 95 (1984).
[24] J. D. Goddard, Chem. Phys. Lett. **102**, 224 (1983).
[25] S. A. Perera, J. D. Watts, and R. J. Bartlett, J. Chem. Phys. **100**, 1425 (1994).
[26] B. Fernández, P. Jørgensen, and J. Simons, J. Phys. Chem. **98**, 7012 (1993).
[27] S. S. Wesolowski, E. M. Johnson, M. L. Leininger, T. D. Crawford, and H. F. Schaefer, J. Chem. Phys. **109**, 2694 (1998).
[28] J. W. Gauld, L. A. Eriksson, and L. Radom, J. Phys. Chem. **101**, 1352 (1997).
[29] L. A. Eriksson, O. L. Malkina, V. G. Malkin, and D. R. Salahub, J. Chem. Phys. **100**, 5066 (1994).
[30] M. T. Nguyen, S. Creve, L. A. Eriksson, and L. G. Vanquickenborne, Mol. Phys. **91**, 537 (1997).
[31] L. A. Eriksson, Mol. Phys. **91**, 827 (1997).
[32] D. Feller and E. R. Davidson, J. Chem. Phys. **80**, 1006 (1984).
[33] D. Feller and E. R. Davidson, Theor. Chim. Acta **68**, 57 (1985).
[34] D. M. Chipman, J. Phys. Chem. **71**, 761 (1979).
[35] C. J. Cramer and M. H. Lim, J. Phys. Chem. **98**, 5024 (1994).
[36] D. Feller, J. Chem. Phys. **93**, 579 (1990).
[37] S. N. Beck, E. A. McCullough, and D. Feller, Chem. Phys. Lett. **175**, 629 (1990).
[38] D. M. Chipman, I. Carmichael, and D. Feller, J. Chem. Phys. **95**, 4702 (1991).
[39] D. Feller, E. D. Glendening, E. A. McCullough, and R. J. Miller, J. Chem. Phys. **99**, 2829 (1993).
[40] B. Chen and M. Huang, Chem. Phys. Lett. **308**, 256 (1999).
[41] B. Webster, J. Chem. Soc., Faraday Trans. **94**, 1385 (1998).
[42] B. J. Krohn, W. C. Ermler, and C. W. Kern, J. Chem. Phys. **60**, 22 (1974).
[43] W. Weltner, *Magnetic Atoms and Molecules* (Van Nostrand Reinhold, New York, 1983).
[44] H. Nakatsuji and M. Izawa, J. Phys. Chem. **91**, 6205 (1989).
[45] S. M. Poling, E. R. Davidson, and G. Vincow, J. Phys. Chem. **54**, 3005 (1971).
[46] K. Raghavachari, G. W. Trucks, J. A. Pople, and M. Head-Gordon, Chem. Phys. Lett. **157**, 479 (1989).
[47] R. J. Bartlett, J. D. Watts, S. A. Kucharski, and J. Noga, Chem. Phys. Lett. **165**, 513 (1990).
[48] R. J. Bartlett, J. D. Watts, S. A. Kucharski, and J. Noga, Chem. Phys. Lett. **167**, 609 (1990).
[49] J. Gauss, W. J. Lauderdale, J. F. Stanton, J. D. Watts, and R. J. Bartlett, Chem. Phys. Lett. **182**, 207 (1991).
[50] A. D. Becke, J. Chem. Phys. **98**, 5648 (1993).
[51] C. Lee, W. Yang, and R. G. Parr, Phys. Rev. B **37**, 785 (1988).
[52] S. Huzinaga, J. Chem. Phys. **42**, 1293 (1965).
[53] T. H. Dunning, Jr., J. Chem. Phys. **53**, 2823 (1970).
[54] T. H. Dunning, Jr. and P. J. Hay, in *Modern Theoretical Chemistry*, edited by H. F. Schaefer (Plenum, New York, 1977), Vol. 3, p. 1.
[55] T. H. Dunning, Jr., J. Chem. Phys. **90**, 1007 (1989).
[56] D. E. Woon and T. H. Dunning, Jr., J. Chem. Phys. **98**, 1358 (1993).
[57] T. H. Dunning, Jr., J. Chem. Phys. **55**, 716 (1971).
[58] R. Krishnan, J. S. Binkley, R. Seeger, and J. A. Pople, J. Chem. Phys. **72**, 650 (1980).
[59] A. D. McLean and G. S. Chandler, J. Chem. Phys. **72**, 5639 (1980).
[60] M. J. Frisch, J. A. Pople, and J. S. Binkley, J. Chem. Phys. **80**, 3265 (1984).
[61] T. Clark, J. Chandrasekhar, and P. v. R. Schleyer, J. Comput. Chem. **4**, 294 (1983).
[62] J. S. Binkley, J. A. Pople, and W. J. Hehre, J. Am. Chem. Soc. **102**, 939 (1980).
[63] M. S. Gordon, J. S. Binkley, J. A. Pople, W. J. Pietro, and W. J. Hehre, J. Am. Chem. Soc. **104**, 2797 (1983).
[64] W. J. Hehre, R. Ditchfield, and J. A. Pople, J. Chem. Phys. **56**, 2257 (1972).
[65] M. M. Francl, W. J. Pietro, W. J. Hehre, J. S. Binkley, M. S. Gordon, and J. A. Pople, J. Chem. Phys. **77**, 3654 (1982).
[66] K. A. Peterson and T. H. Dunning, Jr. (unpublished).
[67] J. Gauss, J. F. Stanton, and R. J. Bartlett, J. Chem. Phys. **95**, 2639 (1991).
[68] J. D. Watts, J. Gauss, and R. J. Bartlett, Chem. Phys. Lett. **200**, 1 (1992).
[69] J. D. Watts, J. Gauss, and R. J. Bartlett, J. Chem. Phys. **98**, 8718 (1993).
[70] ACES II, J. F. Stanton, J. Gauss, W. J. Lauderdale, J. D. Watts, and R. J. Bartlett. The package also contains modified versions of the MOLECULE Gaussian integral program of J. Almlöf and P. R. Taylor, the ABACUS integral derivative program written by T. U. Helgaker, H. J. Aa. Jensen, P. Jørgensen and P. R. Taylor, and the PROPS property evaluation integral code of P. R. Taylor.
[71] GAUSSIAN 94, Revision C.3, M. J. Frisch, G. W. Trucks, H. B. Schlegel, P. M. W. Gill, B. G. Johnson, M. A. Robb, J. R. Cheeseman, T. Keith, G. A. Petersson, J. A. Montgomery, K. Raghavachari, M. A. Al-Laham, V. G. Zakrzewski, J. V. Ortiz, J. B. Foresman, J. Cioslowski, B. B. Stefanov, A. Nanayakkara, M. Challacombe, C. Y. Peng, P. Y. Ayala, W. Chen, M. W. Wong, J. L. Andres, E. S. Replogle, R. Gomperts, R. L. Martin, D. J. Fox, J. S. Binkley, D. J. Defrees, J. Baker, J. J. P. Stewart, M. Head-Gordon, C. Gonzalez, and J. A. Pople, Gaussian, Inc., Pittsburgh, PA, 1995.
[72] C. Ochsenfeld, R. I. Kaiser, Y. T. Lee, and M. Head-Gordon, J. Chem. Phys. **110**, 9982 (1999).
[73] L. A. Eriksson and A. Laaksonsen, J. Chem. Phys. **105**, 8195 (1996).
[74] J. Senekowitsch, S. Carter, P. Rosmus, and H. J. Werner, Chem. Phys. **147**, 281 (1990).
[75] L. A. Curtiss, R. H. Nobes, J. A. Pople, and L. Radom, J. Chem. Phys. **97**, 6766 (1992).
[76] M. Izuha, S. Yamamoto, and S. Saito, J. Mol. Struct. **413**, 527 (1997).
[77] F. X. Brown, S. Yamamoto, and S. Saito, J. Mol. Struct. **412**, 537 (1997).
[78] J. A. Austin, D. H. Levy, C. A. Gottlieb, and H. E. Radford, J. Phys. Chem. **60**, 207 (1974).